J. Fluid Mech. (1968), *vol.* 33, *part* 3, *pp.* 591–616
Printed in Great Britain

Numerical and experimental investigations of the shear layer between two parallel streams

By R. D. MILLS
Engineering Department, Cambridge University

(Received 19 January 1968)

The first-order laminar shear layer between two parallel streams has been calculated exactly for compressible and incompressible two-dimensional flow. Turbulent flow has been included by using Prandtl's hypothesis for the eddy viscosity. Results are presented for a wide range of the appropriate parameters. The problem is solved by writing the momentum and energy equations as a pair of coupled integral equations in Crocco variables; these are solved by the method of successive approximation after using a simple transformation to weaken the singularity at the outer edges of the boundary layer. This approach yields uniquely the shear stress and temperature as functions of the tangential velocity u. The so-called third boundary condition, derived by Ting (1959), is then readily satisfied in evaluating the transverse component of velocity v by quadrature. Experimental results are presented in the turbulent incompressible case. Good agreement with the exact theoretical results is obtained when one stream is much faster than the other, but this falls off as the speeds of the streams tend to equalize.

1. Introduction

The free shear layer formed between two semi-infinite parallel streams of fluid has been the subject of considerable investigation, both theoretical and experimental. Laminar flow in this layer displays a marked instability to small disturbances (see, for example, Lessen 1949) and consequently in practice this layer is almost invariably turbulent. The laminar problem might then have assumed the position of an interesting yet difficult non-linear boundary-value problem were it not for the fact that by the aid of an apparent or eddy coefficient of viscosity it is possible to pose, with trivial mathematical differences, the turbulent problem alongside the laminar problem. Approximate solutions derived on the basis of an apparent viscosity coefficient are known to yield a reasonable overall description of the turbulent phenomenon.

An analysis of the plane turbulent 'half-jet' (lower stream at rest) was given by Tollmien (1926) on the basis of Prandtl's mixing length theory. Tollmien succeeded in reducing the problem to the solution of an ordinary third-order linear differential equation for the stream function f in terms of a similarity co-ordinate η. There are, however, only two immediately obvious boundary conditions to apply, namely that the tangential velocity f' should approach the

outer flow speeds U_1, U_2 as $\eta \to \pm\infty$. Tollmien fixed his solution by making the transverse velocity v_1 vanish at the outer edge $\eta \to +\infty$. Later, Kuethe (1935) extended these calculations to the mixing of two streams, using von Kármán's suggestion that the third boundary condition should correspond to zero net transverse force acting on the layer, viz. $U_1 v_1 + U_2 v_2 = 0$. Both of these authors succeeded in obtaining straightforward explicit solutions because of the simple linear differential equation that resulted from the form of the hypothesis used to describe the effects of turbulence. The non-linear laminar flow equation with boundary conditions of this type was still unsolved.

On the basis of the hypothesis put forward by Prandtl that the eddy viscosity ϵ is proportional to x and $U_1 - U_2$, Görtler (1942) worked out a new theory for this problem. This theory brought the turbulent problem (for $f(\eta)$) into coincidence with the laminar problem, in the case of incompressible flow. Görtler solved the problem approximately by use of a power-series expansion in the parameter $\lambda = (U_1 - U_2)/(U_1 + U_2)$. The solution to first order in λ, the 'error function' solution, has become well known throughout the experimental literature of the problem, as it gives a good approximation to the *shape* of the observed mean velocity profiles. By direct numerical integration and also by momentum-integral methods, Lock (1951) calculated the incompressible laminar mixing of two streams of different fluids. Lock rendered the problem unique by setting $f(0) = 0$ and assuming continuity of shear stress at the interface of the streams. Crane (1957) extended Görtler's work to compressible flow, using an expansion procedure involving λ and the temperature parameter $\lambda' = (T_1 - T_2)/(T_1 + T_2)$. Though Crane derived analytical forms for the functions originally computed numerically by Görtler, his results are of limited general usefulness because of poor convergence of the series.

Görtler, Crane and many others who have given solutions have avoided the question of the correct third boundary condition by (conveniently) fixing their solutions so that the line $\eta = 0$ corresponds to the mean speed $\frac{1}{2}(U_1 + U_2)$ of the streams. Lock also avoids the question by use of $f(0) = 0$. There is no *a priori* reason why either of these simplifications should correspond to theoretical (or physical) reality. In incompressible flow (or laminar compressible flow with $\mu \propto T$ and Prandtl number P unity), there exists, in the absence of a third boundary condition, an infinite number of solutions in the (u, η)-plane, the difference between any two being equivalent to a shift of the velocity profile as a whole in the η-direction. Mathematically, if $f(\eta)$ is a solution satisfying the boundary conditions at $\eta = \pm\infty$, then so is $f(\eta + a)$, where a is any constant. In turbulent incompressible flow one then has the freedom to raise or lower the curves bodily so as best to fit the experimental data; good 'agreement' has often been achieved in this way, for the *shape* of the experimental profiles tends to agree reasonably well with that of the theoretical profiles!

The indeterminateness arises from using the ordinary boundary-layer equations instead of the full Navier–Stokes equations when solving this problem. This must have been apparent to von Kármán and Kuethe, and it was clearly recognized by Crane in his (1957) paper. Ting (1959), however, appears to have

been the first to derive the appropriate third boundary condition to within the accuracy of the ordinary (first-order) differential equations of boundary-layer theory, by the now well-known method of matched asymptotic expansions. In essence, the third boundary condition requires that the second-order pressure differences occurring normal to the mixing layer balance across this region. For incompressible flow this means simply that there is zero net transverse force on the mixing layer; stated otherwise, the reactions of the upper and lower parts of this layer corresponding to their deflexions perpendicular to x are equal and opposite. For compressible flow the final conditions are conceptually more complicated.

While Ting's work has resolved the indeterminateness, the exact calculation of the mixing boundary layer in the general case remains a problem of some difficulty. A direct numerical approach would require (for the velocity layer) the solution of a third-order non-linear differential equation for $f(\eta)$ with three boundary conditions, involving f and f' at $\eta = \pm\infty$, for which there is no standard solution procedure. Alternatively, in incompressible flow (or laminar compressible flow with $\mu \propto T$ and $P = 1$), the constant a can be determined from any one of the incompressible flow solutions which satisfy the correct boundary conditions on f' at $\eta = \pm\infty$, e.g. the solutions of Lock (see appendix). In the general compressible flow case this procedure will not work, for it is necessary to solve the velocity and thermal problems and impose the third boundary condition simultaneously owing to the coupling of thefields.

Part of the purpose of the present paper has therefore been to obtain some exact numerical solutions to this problem in both the general compressible and incompressible cases. The author's interest in the Crocco forms of the boundary-layer equations (Mills 1966) led him to consider the problem from this point of view; it turns out that this approach has several advantages. For the moment it will be enough to remark that the shear stress function $\tau(x, u)$ can be determined by solving (by iteration) a non-linear integral equation into which are built the two boundary conditions of zero shear stress on either side of the mixing layer. This gives the unique solution for $\tau(x, u)$ in the most general case irrespective of the form of the third boundary condition. The third boundary condition is *later* satisfied, when determining the transverse velocity component v from $\tau(x, u)$ by quadrature.

The present author could not find from diverse experimental results in the literature of this problem a series of tests uncommitted to theories assuming the velocity on the line $\eta = 0$ to be $\frac{1}{2}(U_1 + U_2)$ or to other empiricisms. Consequently he decided to perform an experiment in the turbulent incompressible case to see if the solution determined on the basis of the correct third boundary condition agrees with observation. It was found that there was good agreement for large speed differences but this fell off as the speed differences became small. It must of course be borne in mind that such a comparison involves not only a test of the correctness of the third boundary condition but also a test of the validity of Prandtl's hypothesis in describing the turbulent phenomenon. Nevertheless, the velocities on the line $\eta = 0$ are quite close to the theory for small speed differences as also are the complete mean velocity profiles. There is certainly

no justification from these tests for taking this velocity as $\frac{1}{2}(U_1+U_2)$. It would therefore seem worth while to compare the theoretical results obtained in this paper for compressible flow with a reliable series of experimental tests.

2. Boundary-layer equations

Let u and v be the velocity components in the x- and y-directions ('mean' values being assumed for turbulent flow), and take the origin of co-ordinates O at the point where mixing begins (see figure 1). Further, let $\tau(x,u)$ be the shear stress, and $i = c_pT(x,u)$ the enthalpy per unit mass, where T is the temperature and c_p the constant-pressure specific heat (assumed constant throughout the

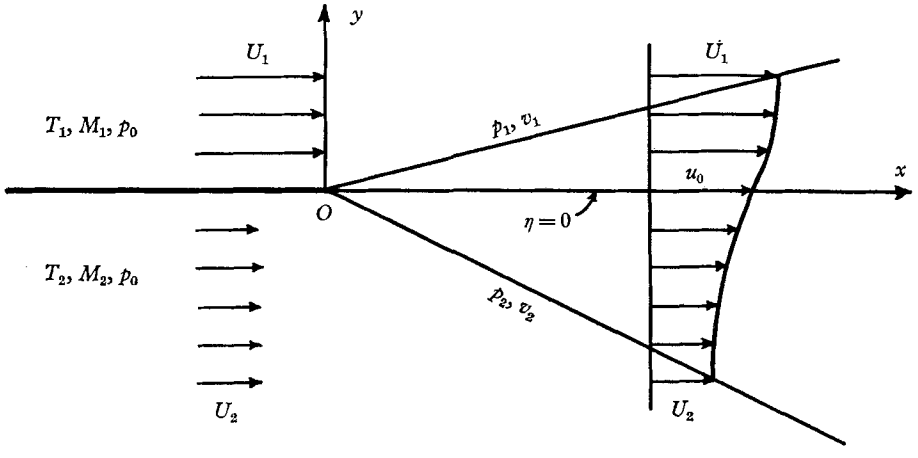

FIGURE 1. Mixing of two semi-infinite streams.

mixing layer). If the pressure p, and i, are independent of x the equations of momentum and energy become in the Crocco formulation (see, for example, Van Driest 1959)

$$\frac{\partial}{\partial x}\left(\frac{\rho^2\epsilon u}{\tau}\right)+\frac{\partial^2\tau}{\partial u^2}=0, \tag{1}$$

$$\tau\left[\frac{d}{du}\left(\frac{1}{P}\frac{di}{du}\right)+1\right]+(1-P)\left(\frac{1}{P}\frac{di}{du}\right)\frac{\partial\tau}{\partial u}=0, \tag{2}$$

where ϵ is the kinematic viscosity coefficient $= \nu = \mu/\rho$ for laminar flow, and represents an apparent or eddy coefficient assumed independent of y when the flow is turbulent. The Prandtl number P equals $c_p\mu/k$ for laminar flow and ϵ/ϵ' for turbulent flow, where $\rho c_p\epsilon'$ is the so-called eddy coefficient of thermal conductivity; μ, ρ, k are respectively the viscosity coefficient, density, and thermal conductivity coefficient of the fluid. The assumption of constant pressure throughout the field (at least to a first-order approximation) implies that

$$\rho \propto T^{-1}, \tag{3}$$

from the perfect-gas law. The viscosity–temperature variation is represented by a power law

$$\mu \propto T^{\omega}, \tag{4}$$

which approximates to observation over a range of temperature dependent on the value of ω, though it would be more accurate to use Sutherland's law for each set of values of the temperatures considered.

It is convenient to work with the non-dimensional variables

$$u^* = (u-U_2)/(U_1-U_2), \quad T^* = (T-T_2)/(T_1-T_2), \tag{5}$$

and to introduce the following parameters characterizing the speed- and temperature-ratios of the streams:

$$\left.\begin{aligned} r &= U_2/U_1, \quad \lambda = (U_1-U_2)/(U_1+U_2), \\ r' &= T_2/T_1, \quad \lambda' = (T_1-T_2)/(T_1+T_2). \end{aligned}\right\} \tag{6}$$

For compressible flow introduce numbers E and W such that

$$E = U^2/c_pT = (\gamma-1)M^2, \quad W = 2E\lambda^2(1+\lambda')/\lambda'(1+\lambda)^2, \tag{7}$$

where M is the Mach number, and γ is the ratio of the constant-pressure and constant-volume specific heats of the fluid.

For laminar flow the condition of similarity implies the following form for τ:

$$\tau = \left[\frac{\mu_1\rho_1(U_1-U_2)^3}{8\lambda x}\right]^{\frac{1}{2}} F(u^*, \lambda, \lambda', \gamma, \omega, P, M_1). \tag{8}$$

On the basis of Prandtl's hypothesis for ϵ,

$$\epsilon = \kappa c x(U_1-U_2),$$

similarity in turbulent flow implies the substitution

$$\tau = \rho_1\sigma\kappa c(U_1-U_2)^2F(u^*, \lambda, \lambda', \gamma, P, M_1), \tag{8'}$$

where σ is Görtler's rate-of-spread parameter, and the constants

$$\kappa, \quad c, \quad \lambda \quad (4\lambda\kappa c\sigma^2 = 1)$$

are taken over from Görtler's (1942) solution. In laminar flow the width of the mixing layer is proportional to $x^{\frac{1}{2}}$, whereas in turbulent flow it is proportional to x, the latter case being depicted in figure 1.

Substitution of (8) or (8') into (1) leads to the following differential equation for F,

$$\frac{d^2F}{du^{*2}} + 2\left[\frac{1+\lambda(2u^*-1)}{F}\right]\left[\frac{1+\lambda'(2T^*-1)}{1+\lambda'}\right]^{\left(\begin{smallmatrix}\omega-1 & 0\\ -2 & 0\end{smallmatrix}\right)} = 0, \tag{9}$$

on utilizing equations (3)–(6). (In the matrix (a_{ij}) denoting the exponent of the non-dimensional temperature function the following convention for the values of the elements is used throughout: a_{11} = laminar compressible, a_{12} = laminar incompressible, a_{21} = turbulent compressible, a_{22} = turbulent incompressible. This device shows at a glance which power should be selected for any of the four given flow types.) The same substitutions in (2) lead to the differential equation

$$\frac{d^2T^*}{du^{*2}} + \left[(1-P)\frac{1}{F}\frac{dF}{du^*}\right]\frac{dT^*}{du^*} = -PW_1, \tag{10}$$

for the thermal problem, on utilizing (7).

The boundary conditions on F and T^* are (see figure 1)

$$(a)\begin{cases} F = 0, & u^* = 0, \\ F = 0, & u^* = 1, \end{cases} \qquad (b)\begin{cases} T^* = 0, & u^* = 0, \\ T^* = 1, & u^* = 1. \end{cases} \tag{11}$$

Condition (a) corresponds to the vanishing of the shear stress at the outer edges of the mixing layer. It should be noted that the present formulation of the problem transfers the parameters λ, λ' (or r, r') from the boundary conditions to the differential equations, which then have a fixed domain of integration.

It is possible to write the boundary-value problems (9), (10), (11) in the form of a coupled pair of integral equations (this technique can in fact be usefully applied to more general problems in boundary-layer theory, see Mills 1966). It will suffice to quote the results; they are obtained by systematically integrating equations (9), (10) with respect to u^* and incorporating the boundary conditions (11) at each step:

$$F(u^*) = (1-u^*)\int_0^{u^*} 2u^* \left[\frac{1+\lambda(2u^*-1)}{F(u^*)}\right]\left[\frac{1+\lambda'(2T^*-1)}{1+\lambda'}\right]^{\begin{pmatrix}\omega-1 & 0\\ -2 & 0\end{pmatrix}} du^* + u^*\int_{u^*}^1 2(1-u^*)\left[\frac{1+\lambda(2u^*-1)}{F(u^*)}\right]\left[\frac{1+\lambda'(2T^*-1)}{1+\lambda'}\right]^{\begin{pmatrix}\omega-1 & 0\\ -2 & 0\end{pmatrix}} du^*, \tag{12}$$

$$T^*(u^*) = \frac{S(u^*)}{S(1)} + PW_1\left[\frac{S(u^*)}{S(1)}R(1) - R(u^*)\right], \tag{13}$$

where

$$S(u^*) = \int_0^{u^*} [F(u^*)]^{P-1} du^*, \quad R(u^*) = \int_0^{u^*} [F(u')]^{P-1}\left\{\int_0^{u'} [F(u)]^{1-P} du\right\} du'.$$

These integrated forms can be checked to satisfy the boundary conditions (11) on inspection, and to satisfy the original differential equations (9), (10) on differentiation. In general, each of the F, T^*, R, S will be functions of u^*, λ, λ', γ, ω, P, M_1 as written out in full in (8), though the dependence on the parameters is not thereafter explicitly displayed. Equations (12) and (13) are coupled for compressible flow, unless $\omega = 1$ in the laminar case.

The usefulness of the present formulation of the problem lies in providing a convenient algorithm for obtaining exact numerical solutions. This idea was first utilized by Crocco (1946) in his work on compressible flat plate boundary-layer flows. If the right-hand sides of (12), (13) are regarded as functions ϕ_1, ϕ_2 of F, T^* then the following iterative scheme may be used to solve these equations,

$$\left.\begin{aligned} F^{(p)}(u^*) &= \phi_1\{F^{(p-1)}(u^*), T^{*(p-1)}(u^*)\}, \\ T^{*(p)}(u^*) &= \phi_2\{F^{(p)}(u^*)\}. \end{aligned}\right\} \tag{14}$$

A difficulty arises, however, in carrying out actual computations, for the differential equation (9) with boundary conditions (11a), or the integral equation (12), has singularities of the type $\xi[\log(1/\xi)]^{\frac{1}{2}}$ at the outer edges of the mixing layer, corresponding to $u^* = 0$ and $u^* = 1$. One can ignore these altogether, or alternatively use the analytical solution in the neighbourhood of $\xi = 0$ and join it to the solution obtained by iteration. The joining process is not trivial however (see Crocco 1946). Another approach is to employ a transformation of the inde-

pendent variable which *weakens* the singularities at the outer edges of the boundary layer, with a consequent improvement in numerical work. The equations (12), (13) are written in terms of the new independent variable s defined by

$$u^* = 3s^2 - 2s^3. \tag{15}$$

The behaviour of $F(s)$ in the neighbourhood of the singularities is now

$$F(s) \sim (3s^2 - 2s^3)[\log(1/(3s^2 - 2s^3))]^{\frac{1}{2}}, \tag{16}$$

which is *less singular* than before in the sense that dF/ds vanishes at $s = 0$, 1, whereas dF/du^* is infinite at $u^* = 0$, 1. The singularities are still 'ignored' in that the extreme mesh points are taken at negligible distances, say 10^{-10}, from the singularities themselves. This technique, however, yields significantly improved numerical results compared with those obtained in a similar manner from the untransformed equation in the case of the well-known 'similarity' flows of ordinary boundary-layer theory (Mills 1966). Consequently this approach was adopted for the present problem, though for clarity the development in terms of u^* is retained throughout the text. As regards the integration formulae used to compute the integrals in (12), (13), it was found that the Simpson rule used once on a given mesh, size h, provided an accuracy comparable to that obtainable from the trapezium rule on meshes of size $4h$, $2h$, h and extrapolating by Aitken's formula. The Simpson rule was thus used for the present problem, though it must be borne in mind that after each iteration this involves the calculation of the values of the iterates at the odd mesh points by interpolation. Almost any plausible solution can be used to start the iteration process, which converges rapidly if the arithmetic means of successive iterates are used as the next starting values ('under-relaxation'). For simplicity $F^{(0)}(s) = s - s^2$, $T'^{*(0)} = s$ were used as starting solutions.

3. The third boundary condition

The other useful feature of the present formulation is that it is possible to separate the problem of the imposition of the third boundary condition from the problem of solving the momentum and energy equations even in the most general case. The third boundary condition involves the normal component of velocity v, which is determined by quadrature subsequent to solving equations (12) and (13); for

$$\left.\begin{aligned} v(x,u) &= u\frac{\partial y(x,u)}{\partial x} + \frac{1}{\rho}\frac{\partial \tau(x,u)}{\partial u}, \\ y(x,u) &= \int_{u_0}^{u} \frac{\rho\epsilon}{\tau(x,u)}\,du, \end{aligned}\right\} \tag{17}$$

where u_0, the velocity on $y = 0$, has to be determined from the third boundary condition. If they had approached the problem from the present point of view, Görtler and Crane would at this stage have set (arbitrarily) $u_0 = \frac{1}{2}(U_1 + U_2)$.

The results of Ting's (1959) investigation to determine the third boundary condition are set out in the first two columns of table 1 for the case of completely

laminar or completely turbulent flow in the mixing layer. The first-order transverse velocities at the upper and lower edges of the mixing layer are denoted by v_1 and v_2 respectively. The simple and obvious extension has been made to the case where the densities of the streams are different.

Nature of streams	Third boundary condition	α	β
(1) Incompressible flow, both streams	$\rho_1 U_1 v_1 + \rho_2 U_2 v_2 = 0$	r	1
(2) Compressible flow, both streams supersonic	$\rho_1 U_1 v_1 (M_1^2-1)^{\frac{1}{2}} + \rho_2 U_2 v_2 (M_2^2-1)^{\frac{1}{2}} = 0$	$\frac{r}{r'}\left(\frac{M_2^2-1}{M_1^2-1}\right)^{\frac{1}{2}}$	r'
(3) Compressible flow, stream 1 supersonic, stream 2 subsonic	$v_1 = 0$	—	—

TABLE 1

Ting's paper should be consulted for the details. It will suffice here to remark that Ting derives conditions (2) and (3) by assuming the terms of order $R^{-\frac{1}{2}}$ in the expansion of the flow *outside* the mixing layer to be governed by the equations of linearized irrotational compressible flow. (R is the expansion Reynolds number as defined in Ting's paper.) To establish a result for subsonic flow in both streams, Ting is obliged to carry on to terms of order $R^{-\frac{3}{2}}$ in the expansion of the flow *inside* the mixing layer, the terms of order R^{-1} vanishing as in incompressible or subsonic flow past a semi-infinite flat plate. For simplicity Ting utilizes the y-component of the Navier–Stokes equation for incompressible flow in his analysis. This may be too drastic a simplification for an essentially compressible flow calculation and Ting's condition for subsonic flow in both streams may be in error; consequently no subsonic flow results were computed, though no additional difficulty would be encountered in satisfying the appropriate condition by the present methods.

When (8) and (8′) are substituted in (17) and the integral equation (12) is differentiated to obtain expressions for $dF(0)/du^*$ and $dF(1)/du^*$, the third boundary condition becomes

$$(1+\lambda)\eta(1,u_0^*) - \int_0^1 u^* G(u^*)\,du^* + \alpha\left\{(1-\lambda)\eta(0,u_0^*) + \beta\int_0^1 (1-u^*)\,G(u^*)\,du^*\right\} = 0, \tag{18}$$

where
$$G(u^*) = \left[\frac{1+\lambda(2u^*-1)}{F}\right]\left[\frac{1+\lambda'(2T^*-1)}{1+\lambda'}\right]^{\begin{pmatrix}\omega-1 & 0\\ -2 & 0\end{pmatrix}},$$

and the similarity co-ordinate η is obtained from (4)–(8) and (17) as

$$\left.\begin{aligned} \eta(u^*,u_0^*) &= \int_{u_0^*}^{u^*}\left[\frac{1+\lambda'(2T^*-1)}{1+\lambda'}\right]^{\begin{pmatrix}\omega & 0\\ -1 & 0\end{pmatrix}}\frac{du^*}{F},\\ \eta &= \frac{y}{\sqrt{x}}\left[\frac{U_1+U_2}{8\nu_1}\right]^{\frac{1}{2}} \quad \text{(laminar flow)}, \quad \eta = \sigma\frac{y}{x} \quad \text{(turbulent flow)}. \end{aligned}\right\} \tag{19}$$

The values of α, β corresponding to the cases (1)–(3) are shown in table 1. Once the functions $F(u^*)$, $T(u^*)$ have been determined, equation (18), say $Z(u_0^*) = 0$, is solved numerically for the velocity u_0^* on the line $\eta = 0$. The co-ordinate $\eta(u^*, u_0^*)$ is then obtained from (19), and the solution to the first-order boundary-layer problem is completely specified.

The local shear stress coefficient and local Nusselt number may be defined as $c_f = \tau/\rho_1(U_1 - U_2)^2$ and $Nu = qx/k_1(T_1 - T_2)$ respectively, where

$$q = -k\partial T/\partial y = -k(dT(u)/du)(\partial u/\partial y)$$

is the local heat transfer rate. From (8), (8′) and (13) it follows that

$$\left.\begin{aligned} C &= F(u^*), \\ N &= [F(u^*)]^P\left[1/S(1) + PW_1\left\{R(1)/S(1) - \int_0^{u^*}[F(u^*)]^{1-P}du^*\right\}\right], \end{aligned}\right\} \tag{20}$$

where $C = 4\lambda\sqrt{(R_{x_0})}\,c_f$, $N = 2Nu/\sqrt{R_{x_0}}$, $R_{x_0} = (U_1 + U_2)x/2\nu_1$ for laminar flow; $C = 2\sqrt{2}\,\lambda\sqrt{(R_{x_0})}\,c_f$, $N = \sqrt{2}\,Nu/\sqrt{R_{x_0}}$, $R_{x_0} = (U_1 + U_2)x/2\epsilon$ for turbulent flow.

The accuracy of the results for a given mesh size h is not uniform over the range of parameters considered in the paper. As a rule results obtained from two mesh sizes h and $\frac{1}{2}h$ were consulted in preparing the tables, h being generally taken as 1/128. For a given h, a slight loss in accuracy occurs (compared with the other boundary-layer characteristics) in calculating $\eta(u^*, u_0^*)$ from (19), for it was necessary to use the trapezium rule to integrate to the nearest even node and then continue using the more accurate Simpson rule. This appears unavoidable without the use of a complicated quadrature scheme. Consequently the use of a very small mesh size was considered to be the best approach for this particular problem as no numerical instabilities were encountered on reducing the mesh size to low values.

4. Incompressible flow

The velocity and thermal problems are uncoupled and (12) may be solved independently of (13) which has $W_1 = 0$. The results of the computations for the velocity distribution are shown graphically in figure 3 for a range of speed-ratios r. There is seen to be a distinct dependence of the solution in the (u^*, η)-plane on the parameter r. As r approaches unity the velocity profiles approach a position of antisymmetry about the line $\eta = 0$. Numerical details of the solution are given in table 2.

Figure 4 shows the temperature distribution as a function of Prandtl number. As in the flow past solid surfaces, the thermal boundary layer becomes progressively thinner compared with the velocity boundary layer as the Prandtl number increases. Note also that the thermal layer is driven more into the lower stream though the position of maximum heat transfer remains constant (see figure 5 and table 3) and depends only on the velocity parameter r. Figure 5 also contains shear stress distributions. It would be instructive to compare these curves with hot-wire measurements of shear stress in the turbulent case.

Experiment

The apparatus used for the experimental investigation of the turbulent mixing of two incompressible streams is shown in figure 2. The apparatus was supplied from a 1000 ft.^{3}/min air-line of inside diameter 4 in. The diffuser and contraction were divided in half by a 1 mm thick splitter plate. Control of the speed-ratio

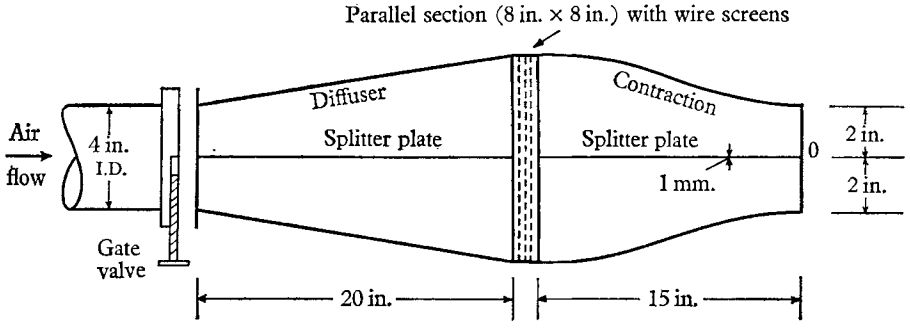

FIGURE 2. Plan view of mixing-layer apparatus.

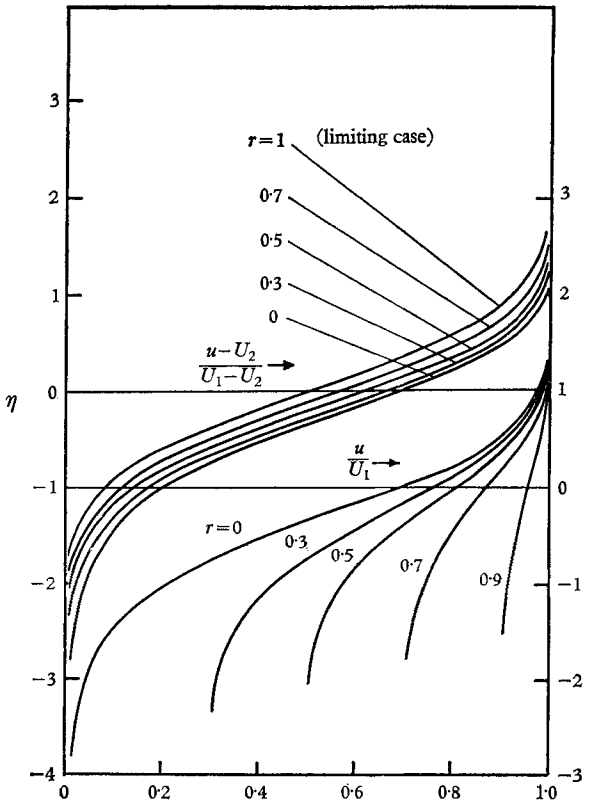

FIGURE 3. Velocity profiles as function of speed-radio r in incompressible flow.

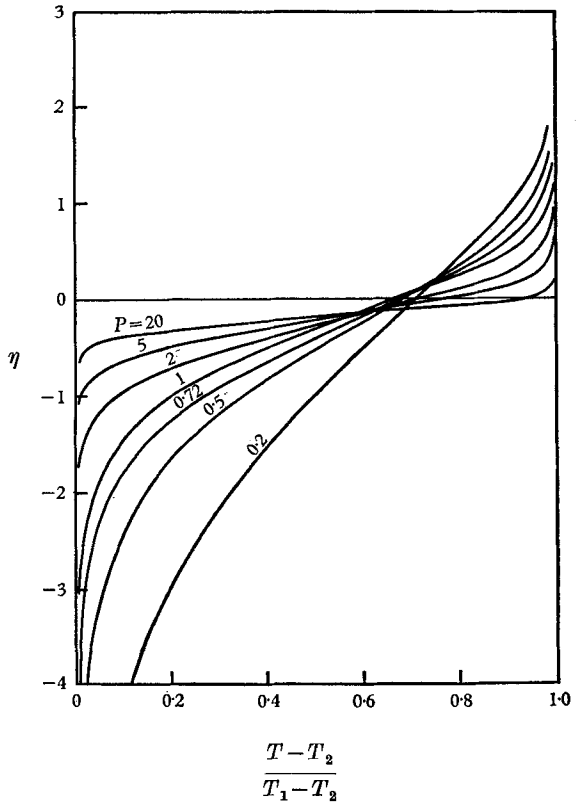

FIGURE 4. Temperature profiles as function of Prandtl number P in incompressible flow.

r	C_m	$\frac{u_m-U_2}{U_1-U_2}$	$-\eta_{C_m}$	$\frac{u_0-U_2}{U_1-U_2}$
0	0·5648	0·5872	0·1871	0·6914
*0	0·5646	0·5873	0·1871	0·6915
0·1	0·5651	0·5720	0·2151	0·6914
0·2	0·5650	0·5592	0·2222	0·6825
0·3	0·5648	0·5482	0·2131	0·6666
0·4	0·5646	0·5385	0·1920	0·6455
0·5	0·5644	0·5301	0·1631	0·6213
0·5014	0·5644	0·5300	0·1627	0·6210
*0·5014	0·5643	0·5301	0·1627	0·6211
0·6	0·5643	0·5226	0·1301	0·5956
0·7	0·5643	0·5160	0·0956	0·5698
0·8	0·5642	0·5101	0·0617	0·5449
0·9	0·5642	0·5048	0·0296	0·5215
1·0	0·5642	0·5	0	0·5

TABLE 2. Mixing-layer characteristics as functions of speed-ratio r in incompressible flow. Suffix m denotes maximum values. * denotes Lock's (1951) values

was effected by a simple gate-valve as shown. The contraction (of ratio 2:1) was designed by a method proposed by the author (Mills 1968). Three wire screens in the parallel section were sufficient to smooth out any large-scale eddying arising from the gate-valve. The aspect ratio of the flows at exit could be varied by the addition of liners contracting the flow in the vertical (z-) direction.

Experiments were made with aspect ratios 3:1 and 2:1 but there was found to be no significant change in the mean velocity profiles arising from this change (see figures 6–9). The velocities were measured by Pitot tube and some measurements were repeated with a 'Disa' constant-temperature hot-wire anemometer (figure 9).

Figures 6–8 show the experimental results compared with the theoretical curves for 3 different speed-ratios. In this comparison it has been necessary to work out from the experimental results a virtual origin (x_0) for the commence-

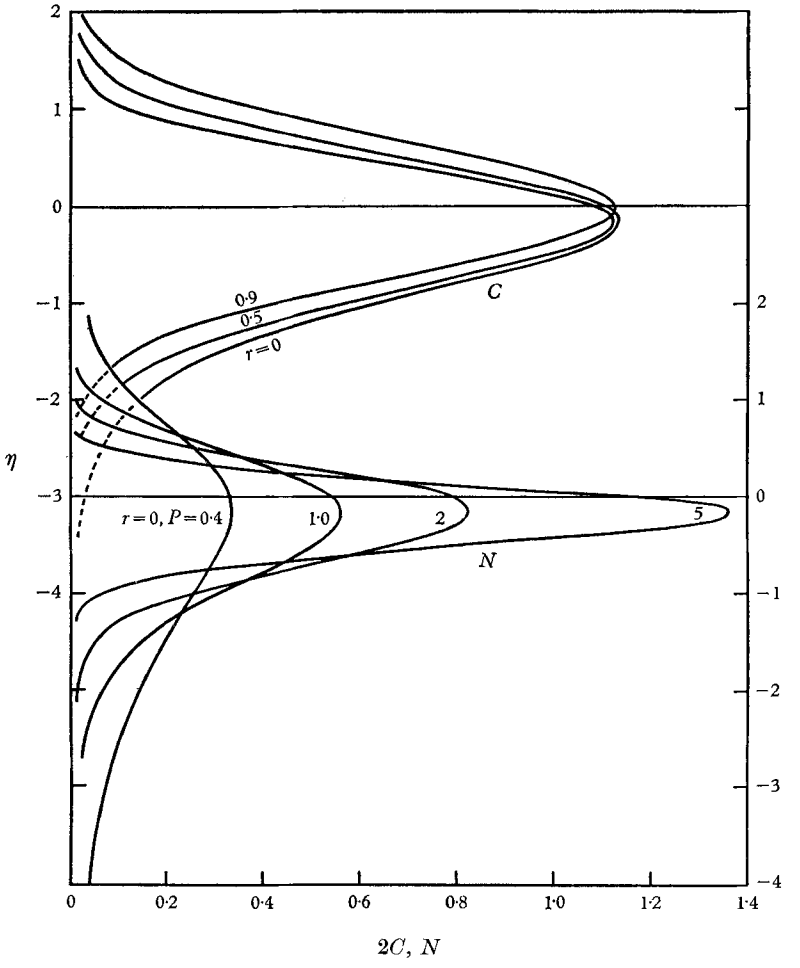

FIGURE 5. Shear stress and local heat transfer distributions across mixing layer in incompressible flow. $C = 4\lambda\sqrt{(R_{x_0})}c_f$, $N = 2Nu/\sqrt{R_{x_0}}$, $R_{x_0} = (U_1+U_2)x/2\nu_1$ laminar flow; $C = 2\sqrt{2}\,\lambda\sqrt{(R_{x_0})}c_f$, $N = \sqrt{2}\,Nu/\sqrt{R_{x_0}}$, $R_{x_0} = (U_1+U_2)x/2\epsilon$ turbulent flow.

	$r = 0$, $\eta_{N_m} = -0{\cdot}1871$		$r = 0{\cdot}5$, $\eta_{N_m} = -0{\cdot}1631$		$r = 0{\cdot}8$, $\eta_{N_m} = -0{\cdot}0617$	
P	N_m	$\frac{T_0-T_2}{T_1-T_2}$	N_m	$\frac{T_0-T_2}{T_1-T_2}$	N_m	$\frac{T_0-T_2}{T_1-T_2}$
0·2	0·227	0·716	0·270	0·591	0·273	0·531
0·4	0·328	0·698	0·359	0·599	0·361	0·535
0·5	0·375	0·694	0·399	0·603	0·401	0·537
0·6	0·418	0·691	0·437	0·607	0·438	0·539
0·72	0·466	0·690	0·478	0·611	0·479	0·541
0·8	0·4962	0·6898	0·5043	0·6144	0·5048	0·5420
1·0	0·5648	0·6914	0·5644	0·6213	0·5642	0·5449
1·2	0·6266	0·6946	0·6190	0·6279	0·6182	0·5475
1·4	0·6831	0·6984	0·6692	0·6341	0·6677	0·5500
2·0	0·8304	0·7117	0·8013	0·6510	0·7983	0·5568
3	1·031	0·7340	0·9830	0·6749	0·9779	0·5665
5	1·345	0·7725	1·271	0·7131	1·263	0·5825
10	1·918	0·8400	1·800	0·7794	1·786	0·6125
20	2·723	0·9136	2·547	0·8579	2·526	0·6546

TABLE 3. Thermal mixing-layer characteristics as functions of Prandtl number P in incompressible flow

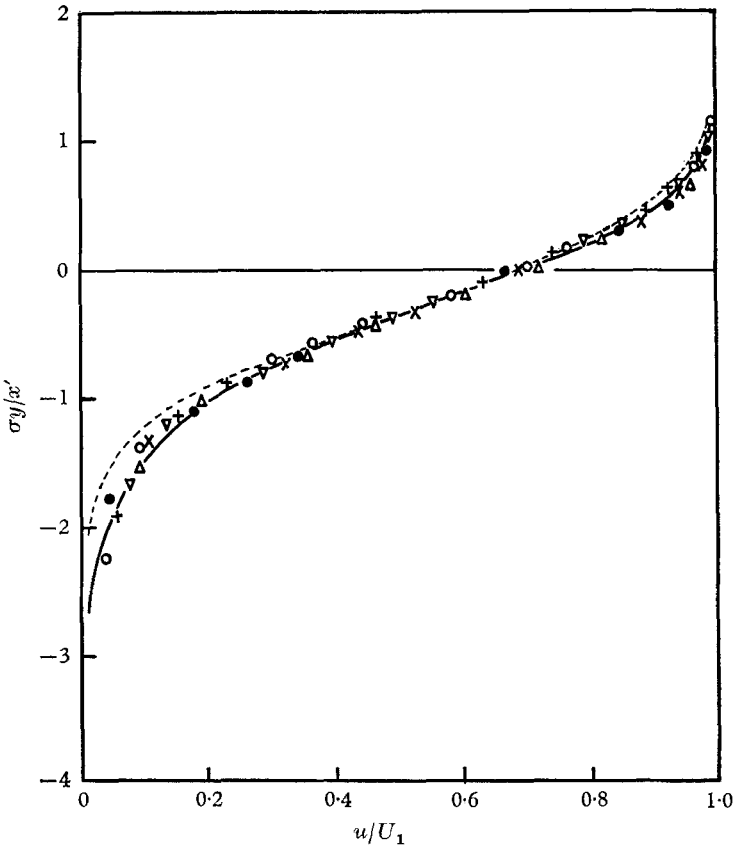

FIGURE 6. Theoretical and experimental velocity profiles for $r = 0$ in turbulent incompressible flow. $AR = 3{:}1$ ($U_1 = 42$ ft./sec at $U_2 = 0$), $\sigma = 10{\cdot}4$, $c = 0{\cdot}135$, $\kappa = 0{\cdot}0171$, $x_0 = -0{\cdot}20$ in. ○, +, ▽ = readings at $x = 4$, 6, 8 in. $AR = 2{:}1$ ($U_1 = 55$ ft./sec at $U_2 = 0$), $\sigma = 10{\cdot}0$, $c = 0{\cdot}141$, $\kappa = 0{\cdot}0178$, $x_0 = -0{\cdot}18$ in. ●, ×, △ = readings at $x = 5$, 7, 9 in. $x' = x$ theory, $x' = x + |x_0|$ experiment. ——, error function.

	C_m		$-\eta_{C_m}$		N_m		$-\eta_{N_m}$		$\frac{u_0-U_2}{U_1-U_2}$		$\frac{T_0-T_2}{T_1-T_2}$	
M_1	Lam.	Turb.	Lam.	Turb.	Lam.	Turb.	Lam.	Turb.	Lam.	Turb.	Lam.	Turb.
1·5	0·5729	0·6423	0·149	0·153	0·497	0·469	0·523	0·649	0·6742	0·6472	0·8547	0·8137
2·0	0·5680	0·6010	0·198	0·195	0·568	0·505	0·718	0·834	0·6958	0·6754	1·003	0·955
*2·0	0·5558	0·5006	0·294	0·263	11·21	7·27	1·262	1·222	0·7302	0·7388	15·33	13·62
3·0	0·5561	0·5108	0·334	0·291	0·809	0·610	1·103	1·09	0·7426	0·7399	1·373	1·297
4·0	0·5428	0·4259	0·517	0·391	1·156	0·724	1·540	1·27	0·7862	0·8016	1·793	1·651
*4·0	0·5348	0·3767	0·606	0·424	42·28	21·00	1·941	1·41	0·8018	0·8308	49·56	40·82
5·0	0·5294	0·3542	0·745	0·485	1·593	0·828	2·055	1·41	0·8229	0·852	2·222	1·962
10·0	0·474	0·159	2·46	0·824	4·904	1·155	5·84	1·82	0·923	0·960	4·06	2·73

TABLE 4. Mixing-layer characteristics as functions of Mach number M_1 in compressible flow. $r = 0$, $r' = 0{\cdot}5$, $\gamma = 1{\cdot}4$, $\omega = 0{\cdot}76$, $P_l = 0{\cdot}72$, $P_t = 0{\cdot}5$. * Computed at $r' = 0{\cdot}99$

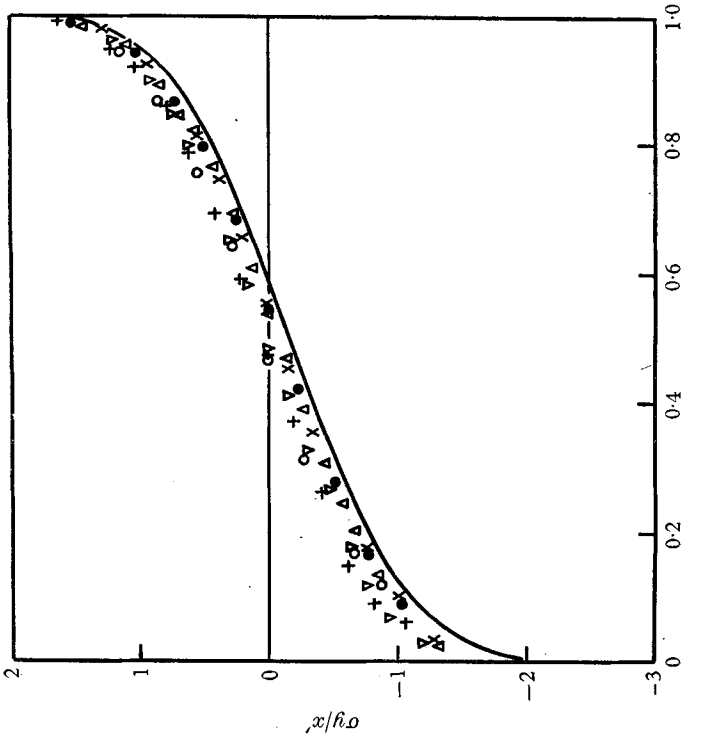

FIGURE 8. Theoretical and experimental velocity profiles for $r = 0.6$ in turbulent incompressible flow. $AR = 3:1$, $\sigma = 25{\cdot}0$, $c = 0{\cdot}059$, $\kappa = 0{\cdot}0273$, $x_0 = -0{\cdot}20$ in. $AR = 2:1$, $\sigma = 26{\cdot}0$, $c = 0{\cdot}056$, $\kappa = 0{\cdot}0262$, $x_0 = -0{\cdot}18$ in.

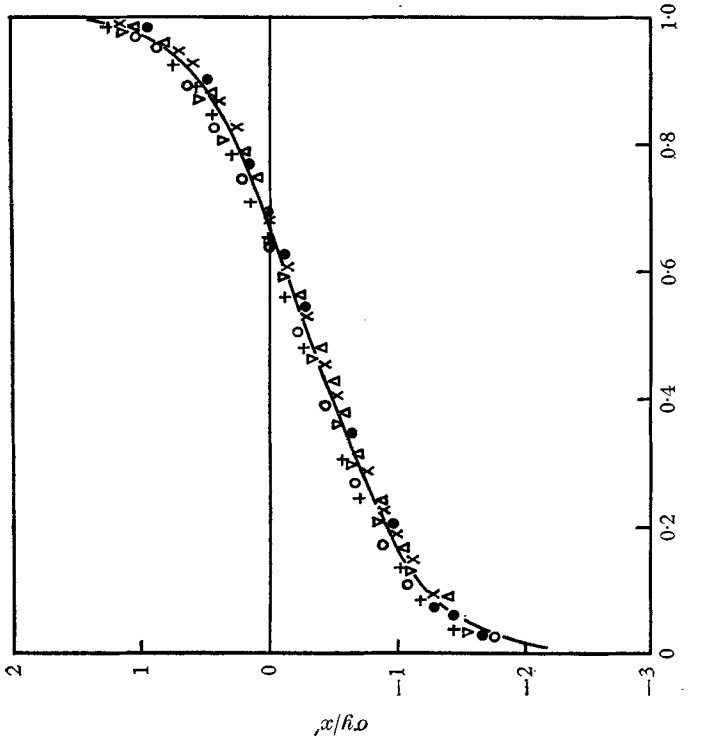

FIGURE 7. Theoretical and experimental velocity profiles for $r = 0.3$ in turbulent incompressible flow. $AR = 3:1$, $\sigma = 18{\cdot}3$, $c = 0{\cdot}078$, $\kappa = 0{\cdot}0178$, $x_0 = -0{\cdot}20$ in., $AR = 2:1$, $\sigma = 16{\cdot}4$, $c = 0{\cdot}087$, $\kappa = 0{\cdot}0198$, $x_0 = -0{\cdot}18$ in.

ment of mixing. In all cases this lay very close to the physical origin O because the ('initial') boundary layers on the splitter plate were very thin as a result of contracting the flow before allowing mixing to take place. The values of the constants σ, κ, c, x_0 are shown in the figures.

In the first two cases the agreement is very good. Note that the exact theoretical solution is somewhat nearer the experimental points than the usual 'error-function' approximation in the extreme parts of the mixing layer for $r = 0$ (figure 6). In this comparison the error-function curve has been placed so as to

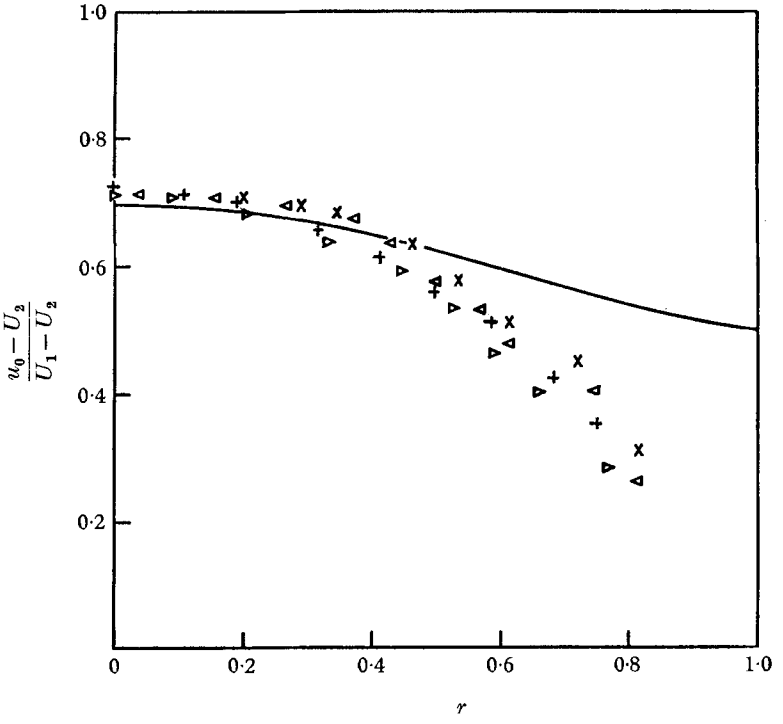

FIGURE 9. Theoretical and experimental velocity distributions on line $\eta = \sigma y/x = 0$ as functions of speed-ratio r in turbulent incompressible flow. $AR = 3:1$, +, ▷ = Pitot, hot-wire readings at $x = 6$ in. $AR = 2:1$, ×, ◁ = Pitot, hot-wire readings at $x = 7$ in.

pass through the correct velocity u_0 given by the exact theory. In the third case $r = 0{\cdot}6$ the experimental points agree well with the shape of the theoretical curve but are displaced somewhat from this curve. This is a symptom of the effect shown in figure 9, where the velocity u_0^* is depicted as a function of r. Agreement is good up to about $r = 0{\cdot}4$; thereafter the experimental points fall below the theoretical curve. It is not clear why this should happen, especially as some care was taken to ensure that the flows were exactly parallel at exit. However, it may simply be that Prandtl's hypothesis is much too simplified a description of the real nature of the turbulent mixing for r near unity.

5. Compressible flow

The velocity and thermal problems are now coupled and it is necessary to iterate equations (12) and (13) in turn to obtain a solution. Apart from this there are no additional difficulties in obtaining solutions, rapid convergence occurring if the iterates are under-relaxed as in the incompressible case.

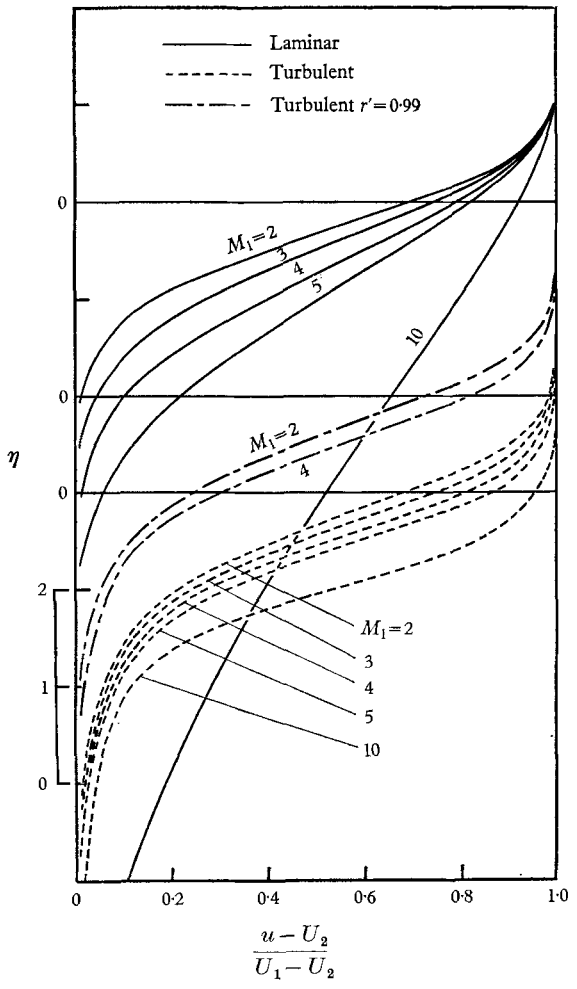

FIGURE 10. Theoretical velocity profiles as functions of Mach number M_1. $r = 0$, $r' = 0{\cdot}5$, $\gamma = 1{\cdot}4$, $\omega = 0{\cdot}76$, $P_l = 0{\cdot}72$, $P_t = 0{\cdot}5$. Middle two curves computed at $r' = 0{\cdot}99$.

The effects of Mach number on the flow are depicted in figures 10, 11, where all the other parameters have been held fixed. Even if these were identical the laminar and turbulent flow results would no longer coincide because of the different exponents (arising from the use of Prandtl's hypothesis for turbulent flow) in the non-dimensional temperature function in (12). The laminar flow results were computed with $P_l = 0{\cdot}72$ and the turbulent flow results with

$P_t = 0{\cdot}5$. (The latter figure was chosen on the basis of experimental work by Fage & Falkner (1932) and Reichardt (1944) on free turbulent flow.)

As in the laminar boundary layer on a flat plate the velocity boundary layer thickens and the velocity profiles tend to become linear as M_1 increases. In the turbulent case, the velocity profiles tend to crowd together near the lower

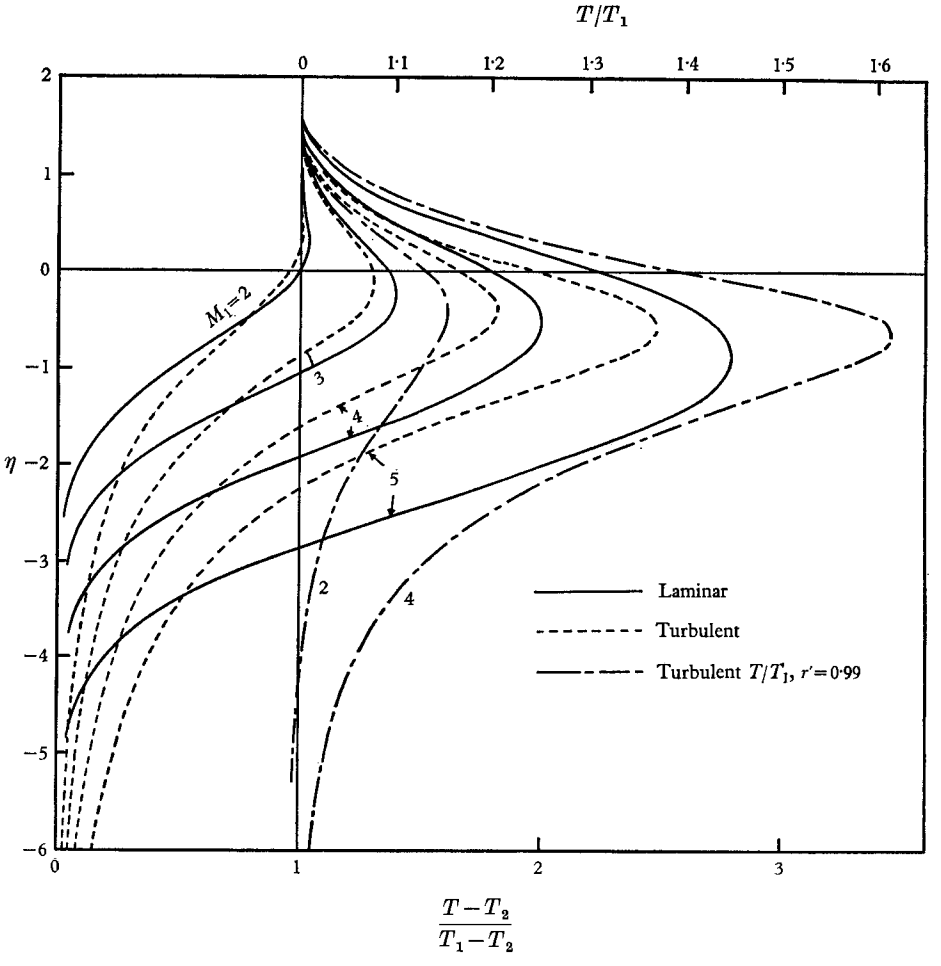

FIGURE 11. Theoretical temperature profiles as functions of Mach number M_1. $r = 0$, $r' = 0{\cdot}5$, $\gamma = 1{\cdot}4$, $\omega = 0{\cdot}76$, $P_l = 0{\cdot}72$, $P_t = 0{\cdot}5$. T/T_1 curves computed at $r' = 0{\cdot}99$.

edge of the mixing region. This difference has its origin in the large difference in the values of the exponents of the non-dimensional temperature function. In both cases, however, the mixing layer is driven progressively into the lower stream as M_1 increases. In the temperature field (figure 11) significant frictional heating does not occur for values of M_1 below about 2; thereafter, this effect steadily increases. This source of heat has the effect of reversing the direction of the net heat flux in the upper part of the mixing layer. Also included in figures 10, 11 and in table 4 are the cases of nearly isothermal ($r' = 0{\cdot}99$) turbulent mixing at $M_1 = 2$ and 4. These cases could readily be compared with experiment.

	C_m		$-\eta c_m$		N_m		$-\eta_{Nm}$		$\frac{u_0-U_2}{U_1-U_2}$		$\frac{T_0-T_2}{T_1-T_2}$	
r	Lam.	Turb.	Lam.	Turb.	Lam.	Turb.	Lam.	Turb.	Lam.	Turb.	Lam.	Turb.
0	0·5428	0·426	0·517	0·391	1·156	0·724	1·54	1·27	0·786	0·802	1·793	1·65
0·3	0·5608	0·560	0·256	0·212	0·863	0·758	0·903	0·903	0·673	0·639	1·282	1·159
0·5	0·5711	0·648	0·036	−0·022	0·660	0·661	0·489	0·528	0·546	0·481	0·897	0·776
0·7	0·5792	0·725	−0·109	−0·187	0·530	0·576	0·135	0·147	0·442	0·373	0·579	0·493
0·9	0·5840	0·774	−0·163	−0·260	0·497	0·553	−0·130	−0·210	0·385	0·324	0·415	0·359

TABLE 5. Mixing-layer characteristics as functions of speed-ratio r in compressible flow. $r' = 0{\cdot}5$, $\gamma = 1{\cdot}4$, $\omega = 0{\cdot}76$, $P_l = 0{\cdot}72$, $P_t = 0{\cdot}5$, $M_1 = 4$

	C_m		$-\eta C_m$		N_m		$-\eta N_m$		$\frac{u_0-U_2}{U_1-U_2}$		$\frac{T_0-T_2}{T_1-T_2}$	
r'	Lam.	Turb.	Lam.	Turb.	Lam.	Turb.	Lam.	Turb.	Lam.	Turb.	Lam.	Turb.
0·2	0·5486	0·473	0·462	0·365	0·855	0·639	1·324	1·187	0·775	0·774	1·419	1·327
0·4	0·5446	0·439	0·499	0·383	1·021	0·674	1·466	1·240	0·783	0·794	1·628	1·512
0·6	0·5410	0·414	0·536	0·398	1·362	0·812	1·617	1·294	0·790	0·809	2·039	1·857
0·8	0·5377	0·393	0·572	0·412	2·403	1·304	1·777	1·350	0·796	0·821	3·262	2·865

TABLE 6. Mixing-layer characteristics as functions of temperature-ratio r' in compressible flow.
$r = 0$, $\gamma = 1{\cdot}4$, $\omega = 0{\cdot}76$, $P_l = 0{\cdot}72$, $P_t = 0{\cdot}5$, $M_1 = 4$

	C_m		$-\eta_{C_m}$		N_m		$-\eta_{N_m}$		$\frac{u_0-U_2}{U_1-U_2}$		$\frac{T_0-T_2}{T_1-T_2}$	
P	Lam.	Turb.	Lam.	Turb.	Lam.	Turb.	Lam.	Turb.	Lam.	Turb.	Lam.	Turb.
0·2	0·552	0·472	0·424	0·355	0·440	0·392	1·66	1·45	0·776	0·780	1·44	1·41
0·4	0·546	0·435	0·497	0·389	0·736	0·617	1·64	1·32	0·790	0·799	1·65	1·60
0·6	0·5438	0·419	0·514	0·391	1·007	0·826	1·58	1·22	0·788	0·802	1·748	1·693
0·8	0·5423	0·4087	0·519	0·388	1·250	1·014	1·519	1·151	0·785	0·803	1·818	1·760
1·0	0·5412	0·4005	0·522	0·385	1·471	1·184	1·474	1·097	0·7820	0·8038	1·873	1·813
1·2	0·5404	0·3937	0·525	0·383	1·672	1·338	1·438	1·054	0·7795	0·8044	1·917	1·856
2·0	0·5382	0·3736	0·532	0·375	2·353	1·863	1·344	0·940	0·7726	0·8078	2·038	1·967

TABLE 7. Mixing-layer characteristics as functions of Prandtl number P in compressible flow.
$r = 0$, $r' = 0{\cdot}5$, $\gamma = 1{\cdot}4$, $\omega = 0{\cdot}76$, $M_1 = 4$

Figures 12, 13 show the effect of varying the speed-ratio r with all the other parameters fixed. In this case conditions (2) and (3) in table 1 are covered as r increases from zero. As the speeds of the streams tend to equalize the mixing

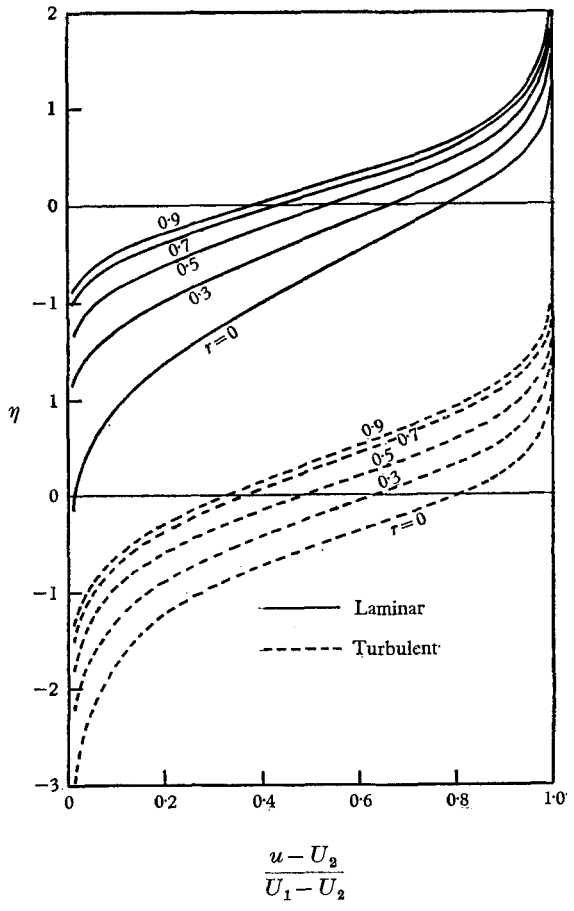

FIGURE 12. Theoretical velocity profiles as functions of speed-ratio r. $r' = 0{\cdot}5$, $\gamma = 1{\cdot}4$, $\omega = 0{\cdot}76$, $P_l = 0{\cdot}72$, $P_t = 0{\cdot}5$, $M_1 = 4$.

ω	C_m	$-\eta_{Cm}$	N_m	$-\eta_{Nm}$	$\frac{u_0-U_2}{U_1-U_2}$	$\frac{T_0-T_2}{T_1-T_2}$
0·50	0·5202	0·495	1·117	1·477	0·789	1·785
0·75	0·5419	0·517	1·155	1·538	0·786	1·792
1·00	0·5648	0·539	1·194	1·602	0·784	1·800
1·25	0·5890	0·563	1·237	1·670	0·781	1·808
1·50	0·6146	0·588	1·282	1·742	0·779	1·815
2·00	0·6700	0·642	1·380	1·90	0·774	1·830

TABLE 8. Mixing-layer characteristics as functions of temperature exponent ω in laminar compressible flow. $r = 0$, $r' = 0{\cdot}5$, $\gamma = 1{\cdot}4$, $P_l = 0{\cdot}72$, $M_1 = 4$

layer moves more into the upper stream; in fact $M_2 > M_1$ for $r > \sqrt{2}/2$ with $r' = 0{\cdot}5$. Little frictional heat is generated within the thermal layer until r becomes less than about 0·5. The mixing-layer characteristics are given quantitatively in table 5.

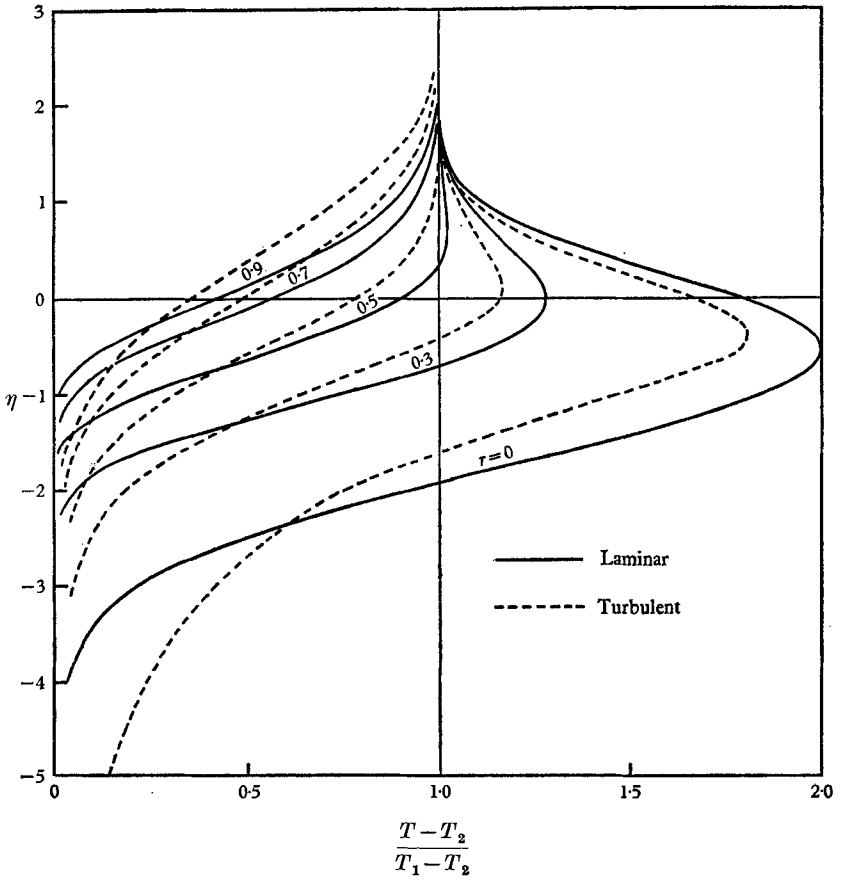

FIGURE 13. Theoretical temperature profiles as functions of speed-ratio r. $r' = 0{\cdot}5$, $\gamma = 1{\cdot}4$, $\omega = 0{\cdot}76$, $P_l = 0{\cdot}72$, $P_t = 0{\cdot}5$, $M_1 = 4$.

r	r'	M_1	A	C_m	$-\eta_{C_m}$	N_m	$-\eta_{N_m}$	$\frac{u_0-U_2}{U_1-U_2}$	$\frac{T_0-T_2}{T_1-T_2}$
0	0·5	4	1·10	0·5648	0·545	1·521	1·538	0·7791	1·880
*0	0·5	4	1·10	0·5646	0·547	1·522	1·541	0·7791	1·881
0·5014	0·8	4	0·388	0·5644	0·187	1·275	0·795	0·6241	1·557
*0·5014	0·8	4	0·388	0·5643	0·186	1·276	0·798	0·6241	1·557

TABLE 9. Comparison of laminar compressible mixing-layer characteristics with those derived from Lock's (1951) results* for $\gamma = 1{\cdot}4$, $\omega = 1$, $P_l = 1$

Numerical tests were also made on the effects of the other parameters. As would be expected, the temperature-ratio r' has only a slight effect on the velocity boundary layer (see table 6 and figure 10). The effect of Prandtl number on c_f (table 7) is less pronounced than that of the temperature exponent ω (table 8).

6. Concluding remarks

The problem of the first-order mixing layer between parallel streams is rendered unique by information derived from the higher-order terms in the asymptotic expansion of the full Navier–Stokes equations. The exact calculation of this shear layer in the general case is not straightforward, however. In this paper it has been calculated exactly by an integral equation approach based on Crocco's forms of the boundary-layer equations.

Two-dimensional incompressible turbulent mixing of two streams of air has been investigated experimentally for a range of speed-ratios, and good agreement with the theory has been observed for low values of r. There is no evidence from this experiment for taking the velocity u_0 on the line $\eta = 0$ as $\frac{1}{2}(U_1 + U_2)$ as has often been done in theoretical investigations. It would therefore be instructive to compare with experiment the theoretical results presented in this paper for turbulent compressible flow.

The author would like to express his indebtedness to Professor W. A. Mair for the interest he has shown in this work and for valuable criticisms of the paper. Thanks are due also to Dr L. C. Squire for valuable comments on the paper. The author is grateful for the use of experimental facilities in the Cambridge University Aeronautics Laboratory, and for the receipt of the necessary computer time on the Cambridge University TITAN computer. This work was made possible by the award of an I.C.I. Fellowship.

Appendix

It is possible to check the present results against those obtained by Lock (1951) in certain special cases. This is quite straightforward in incompressible flow. Let the stream function be given by $\psi = (\nu_1 U_1 x)^{\frac{1}{2}} f(\bar{\eta} + a)$, where Lock's similarity co-ordinate is given by $\bar{\eta} = y(U_1/\nu_1 x)^{\frac{1}{2}}$ and a is the unknown constant to be determined by the condition (1) of momentum balancing in table 1. From the asymptotic representations of $f(\bar{\eta} + a)$

$$\left.\begin{aligned} f(\bar{\eta}+a) &\sim \bar{\eta}+a+b_1, \\ v_1 &\to -\tfrac{1}{2}(b_1+a)\left(\frac{U_1\nu_1}{x}\right)^{\frac{1}{2}}, \end{aligned}\right\} \quad \bar{\eta}\to\infty, \tag{21a, b}$$

$$\left.\begin{aligned} f(\bar{\eta}+a) &\sim \frac{U_2}{U_1}(\bar{\eta}+a+b_2), \\ v_2 &\to -\frac{1}{2}\frac{U_2}{U_1}(b_2+a)\left(\frac{U_1\nu_1}{x}\right)^{\frac{1}{2}}, \end{aligned}\right\} \quad \bar{\eta}\to-\infty, \tag{22a, b}$$

where b_1 and b_2 are known constants from Lock's solution. The equation to determine a is then simply

$$a(1+r^2) = -b_1 - r^2 b_2. \tag{23}$$

The value of a is immediately obtainable from the present computations as $|\eta_{C_m}| \times 8^{\frac{1}{2}}/(1+r)^{\frac{1}{2}}$, the factor arising from the difference in normalizations. In the case of $r = 0$ this gives $a = 0{\cdot}5292$ compared with $0{\cdot}5289$ from (23) using Lock's solution. Full comparisons are shown in table 2 for $r = 0$ and $r = 0{\cdot}5014$.

For compressible flow it is necessary to employ the Howarth–Dorodnitsyn transformation

$$\psi(x, y) \to \Psi(x, \bar{Y}), \quad \bar{Y} = \int_0^y (\rho/\rho_1)\, dy$$

to effect a comparison. Similarity in compressible flow means the stream function takes the form

$$\Psi = (\nu_1 U_1 x)^{\frac{1}{2}} f(H), \quad H = \bar{H} + A, \quad \bar{H} = \bar{Y}(U_1/\nu_1 x)^{\frac{1}{2}}, \tag{24}$$

and hence

$$u = \partial\Psi/\partial\bar{Y} = U_1 f'(H), \quad T/T_1 = g(H),$$

$$v = -\partial\Psi/\partial x = \frac{1}{2}\left(\frac{\nu_1 U_1}{x}\right)^{\frac{1}{2}} \left[g(H)\{(H-A)f' - f\} - f' \int_A^H (H-A) g'\, dH\right], \tag{25a,b}$$

(see, for example, Stewartson 1964). With the aid of the asymptotic forms (21*a*), (22*a*) the third boundary condition can be written

$$(b_1 + A) + \int_A^\infty (H-A) g'\, dH + \alpha\left[r r'(b_2 + A) + r \int_A^{-\infty} (H-A) g'\, dH\right] = 0, \tag{26}$$

where α is the constant from table 1. This equation must be solved for the unknown constant A and is the equivalent of the present equation (19).

In general it would be necessary to solve the momentum and energy equations simultaneously with satisfying this condition. However, for the case $\omega = 1$, $P = 1$ it is possible to determine the solution completely from Lock's results since $g(H)$ is then a quadratic function of $f'(H)$ (Crocco's law):

$$\frac{T}{T_1} = g(H) = \frac{r' - r}{1 - r} + \frac{1 - r'}{1 - r} f' - \tfrac{1}{2}(\gamma - 1) M_1^2 \{r - (1+r) f' + f'^2\}, \tag{27}$$

which satisfies $T(\infty) = T_1$, $T(-\infty) = T_2$.

Two cases were worked out in detail corresponding to Lock's solutions for $r = 0$ and $r = 0{\cdot}5014$. To avoid solving (26) numerically for A, the value of A is determined from the present solution. This is achieved by interpolating Lock's velocity profiles, for A is the value of $\bar{H}$ where Lock's $u(\bar{H})/U_1$ is equal to u_0/U_1 as determined from the present solution. Equation (26) was then checked with this value of A, and all the other characteristics worked out. In particular, the coordinates η_{C_m}, $\bar{\eta}_{C_m}$ of maximum shear stress are obtained from

$$\left(\frac{8}{1+r}\right)^{\frac{1}{2}} \eta_{C_m} = \bar{\eta}_{C_m} = \int_A^0 g(H)\, dH. \tag{28}$$

The comparison is displayed in full in table 9. Note that the shear stress and local

heat transfer functions in Lock's normalization are smaller than their counterparts in the present paper by the factors $8^{\frac{1}{2}}/(1+r)^{\frac{1}{2}}(1-r)$ and $8^{\frac{1}{2}}/(1+r)^{\frac{1}{2}}(1-r')$ respectively.

Finally, in compressible flow having Prandtl number unity the locus of zero heat transfer ($dT^*/du^* = 0$) can easily be shown from equation (13) to be

$$u_h^* = \frac{1}{2}\left(1+\frac{2}{W_1}\right). \tag{29}$$

A few points determined numerically by the present method were checked to lie on this curve.

REFERENCES

Crane, L. J. 1957 *J. Fluid Mech.* **3**, 81.

Crocco, L. 1946 *Monographie Scientifiche di Aeronautica*, **3**.

Fage, A. & Falkner, V. M. 1932 Appendix to G. I. Taylor, *Proc. Roy. Soc.* A **135**, 685.

Görtler, H. 1942 *ZAMM* **22**, 244.

Kuethe, A. 1935 *J. Appl. Mech.* **2**, A87.

Lessen, M. 1949 *NACA TN* 1929.

Lock, R. C. 1951 *Quart. J. Mech. Appl. Math.* **4**, 42.

Mills, R. D. 1966 *Rept. Memor. aero. Res. Counc., Lond.* no. 3515.

Mills, R. D. 1968 *Aero. Quart.* **19**, 91.

Reichardt, H. 1944 *ZAMM* **24**, 268.

Stewartson, K. 1964 *The Theory of Laminar Boundary Layers in Compressible Fluids.* Oxford University Press.

Ting, L. 1959 *J. Math. Phys.* **38**, 153.

Tollmien, W. 1926 *ZAMM* **6**, 468; *NACA TM* 1085 (1945).

Van Driest, E. R. 1959 Article in C. C. Lin (Ed.) *Turbulent Flows and Heat Transfer*, vol. v, Oxford: Princeton series.